

Evidence for Fermi surface reconstruction in the static stripe phase of $\text{La}_{1.8-x}\text{Eu}_{0.2}\text{Sr}_x\text{CuO}_4$, $x = 1/8$

V. B. Zabolotny,¹ A. A. Kordyuk,^{1,2} D. S. Inosov,¹ D. V. Evtushinsky,¹ R. Schuster,¹ B. Büchner,¹ N. Wizent,¹ G. Behr,¹ Sunseong Pyon,³ H. Takagi,³ R. Follath,⁴ and S. V. Borisenko¹

¹Institute for Solid State Research, IFW-Dresden, PO.Box 270116, D-01171 Dresden, Germany

²Institute of Metal Physics of National Academy of Sciences of Ukraine, 03142 Kyiv, Ukraine

³Engineering Research Institute, University of Tokyo, Yayoi, Bunkyo-ku, Tokyo 113, Japan

⁴BESSY GmbH, Albert-Einstein-Strasse 15, 12489 Berlin, Germany

We present a photoemission study of $\text{La}_{0.8-x}\text{Eu}_{0.2}\text{Sr}_x\text{CuO}_4$ with doping level $x=1/8$, where the charge carriers are expected to order forming static stripes. Though the local probes in direct space seem to be consistent with this idea, there has been little evidence found for such ordering in quasiparticle dispersions. We show that the Fermi surface topology of the 1/8 compound develops notable deviations from that observed for $\text{La}_{2-x}\text{Sr}_x\text{CuO}_4$ in a way consistent with the FS reconstruction expected for the antiphase stripe order.

PACS numbers: 74.72.Dn, 74.25.Jb, 74.81.-g, 79.60.-i

Since the discovery of charge- and spin-ordering in high- T_c cuprates, the phenomenon has attracted much attention, both from the theoretical and experimental point of view [1, 2]. Moreover, there appeared a number of theoretical approaches considering the charge and spin segregation as having strong, if not decisive, impact on the onset of superconductivity in high- T_c superconductors [3, 4]. The ordering effects were found to depend crucially on the charge doping level, being the most pronounced for the pseudogap regime in the vicinity of doping level $x = 1/8$, where the doped holes are expected to form so-called stripes with the antiferromagnetically ordered spins. Generally, the stripe order is supposed to fluctuate, though for particular superconductors like $\text{La}_{2-x-y}\text{M}_x\text{Sr}_y\text{CuO}_4$ ($M = \text{Nd}$ or La) the inhomogeneities were shown to be practically static [5, 6, 7, 8, 9, 10, 11, 12], making those compounds most prevalent in experimental research. The spin response of the stripe phase has been studied in inelastic neutron scattering experiments [12, 13] supporting the idea of spin ordering. Similarly, local probes, such as scanning tunnelling microscopy, have clearly demonstrated charge modulation on the surface of high temperature superconductors [14, 15], changing the hypothesis of spin and charge modulation into a well established fact. On general grounds any charge/spin ordering must act as an additional scattering potential, resulting in a reconstruction of the initial Fermi surface (FS). Indirect evidence for such modifications comes from Hall coefficient and de Haas-van Alphen measurements [16, 17, 18, 19], suggesting a formation of new orbits when the stripe order sets in. Nonetheless the experiments that would explicitly expose the effect of charge stripe order on the free charge carriers, namely modifications to the electronic band dispersion and topology of the FS, are not numerous and suggest radically different distribution of quasiparticle spectral weight over the Brillouin zone [20, 21].

Here we present experimental data on the electronic band structure of $\text{La}_{1.675}\text{Eu}_{0.2}\text{Sr}_{0.125}\text{CuO}_4$ obtained using angle re-

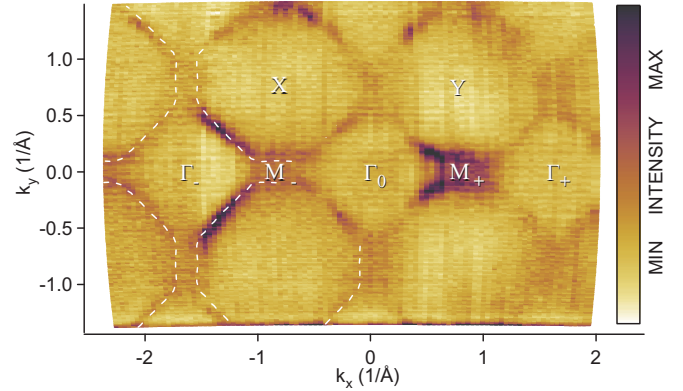


Fig. 1. Experimental FS map of $\text{La}_{1.675}\text{Eu}_{0.2}\text{Sr}_{0.125}\text{CuO}_4$, $T = 25$ K. No symmetrization was applied, the map contains a set of independent \mathbf{k} points covering several Mahan cones [22]. The map was measured with light polarization perpendicular to the analyzer entrance slit, and normalized to the total intensity. Further details on experimental geometry and data processing can be found elsewhere [23, 24, 25].

solved photoelectron spectroscopy (ARPES) and compare the topology of the experimentally observed FS to that of pure $\text{La}_{2-x}\text{Sr}_x\text{CuO}_4$ (LSCO) samples as well as to predictions obtained within a simple model where electrons scatter on effective potential induced by the stripe and charge order. We show that the measured distribution of photoelectron intensity is consistent with the FS reconstruction expected for the antiphase stripe order [26, 27] and give quantitative estimates for the strength of the scattering potential in the spin and charge channels.

The experimental data were collected using 1³ station at the BESSY synchrotron facility with energy and momentum resolution of 12 meV and 0.05\AA^{-1} respectively. The high quality single crystals of $\text{La}_{1.675}\text{Eu}_{0.2}\text{Sr}_{0.125}\text{CuO}_4$ with suppressed superconductivity were mounted on the cryomanipulator and cleaved *in situ* in ultrahigh vacuum. All the data presented in the manuscript were collected at low temperature $T = 25$ K.

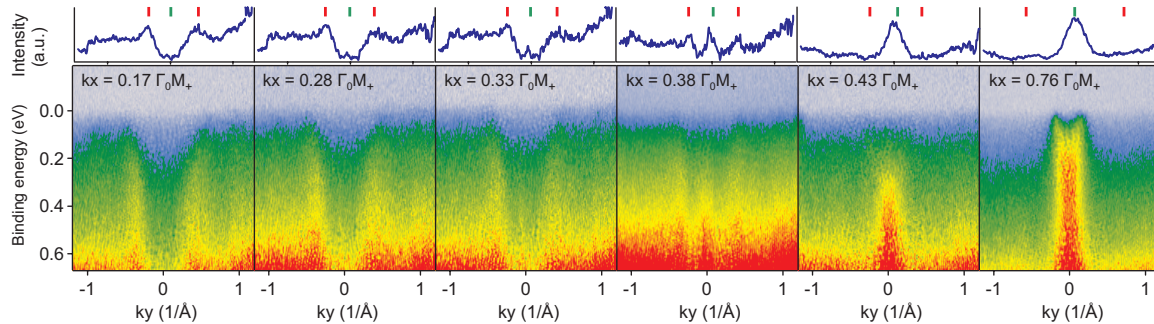


Fig. 2. Evolution of the spectral weight through the Brillouin zone. The curves on top of each energy-momentum image represents an MDC integrated in the energy window 0.3–0.4 eV.

We start the discussion of the experimental data with the FS map plotted in Fig. 1, which represents the photoelectron intensity integrated over a small energy window $E = E_F \pm 15$ meV. While for pure LSCO with the doping level $0.05 \lesssim x \lesssim 0.17$ the FS consists of the rounded contours centered at the X/Y points, for the Eu-doped sample the form of the FS contours is qualitatively different. There are extended and practically straight FS segments passing through the nodal points comprising 45° angle with the primary axes. At the antinodal point the apparent FS contour changes direction, forming segments parallel to the primary crystallographic axes, so that the whole FS rather reminds an octagon as shown by dotted guide lines in Fig. 1.

Assuming that the observed contours represent a true connected FS we tried to fit it with a standard tight-binding (TB) formula [28]. It was practically impossible to find a set of TB parameters that would provide a reasonable fit both at the Fermi level (FL) as well as at higher binding energies. This was the first indirect indication that the assumed topology of the FS is not a true one, in a sense that the apparent FS may consist of several disjoint pockets, which in view of disorder introduced by Eu doping or/and short correlation length of the stripe potential are hard to detect. In some sense the situation may be similar to the electron doped cuprates, whose FS undergoes reconstruction with decreasing the charge doping, though in the photoemission data the reconstructed FS consisting of the hole and electron pockets still resembles the unreconstructed one [29].

Conjecture that the embraced by the guide line area corresponds to the hole doped region would also results in the exaggerated doping $x = 0.19 \pm 0.02$ and thus would be at variance with a reasonable agreement between the nominal doping level of the LSCO system and the one estimated by the FS area [28]. Other, and probably the most straightforward, evidence for the discontinuity of the assumed FS contour comes from the analysis of the photoemission intensity over the whole measured range of binding energies. In Fig. 2 we plot a series of energy-momentum cuts, representing photoelectron intensity for several fixed k_x values spanning from Γ_0 to M_1 point as a function of k_y and binding energy. In the first column one can clearly see two bands crossing the FL at $k_y \approx \pm 0.3 \text{ \AA}^{-1}$. Were the assumed

octagonal FS contours really continuous, one should see these two bands and corresponding FL crossings gradually moving closer to each other as k_x approaches the M point. Indeed the aforementioned FL crossings are getting slightly closer as it follows from the second column of Fig. 2, but at $k_y = 0$ there appears another band that gains the intensity and finally results in a well defined FL crossing for the $k_x \gtrsim 0.6 \Gamma_0 M_+$, i.e. the FS segments at $k_x \lesssim 0.6 \Gamma_0 M_+$ and $k_x \gtrsim 0.6 \Gamma_0 M_+$ must belong to a separate FS sheet and the seeming continuity must be only due to the large momentum width of the features and specifics of the photoemission that make the FS segments that practically coincide with the “parent” FS the most intense and dominating over the replicas in the ARPES signal.

Along with the FS breaking into several sheets one would also expect characteristic for this case backfolding effects in the band dispersions. Nevertheless this kind of reasoning must be exploited cautiously as the coherence length of the folding potential may result in notable deviation from the simple picture. It is well known that the FS of some electron doped cuprates is reconstructed, splitting into the hole and electron pockets [29]. The reason for this reconstruction is likely to be the short range antiferromagnetic correlations that appear for the electron doping $x \lesssim 0.14$. In Fig. 3 (a) we show a typical “backfolded” band for $\text{Pr}_{1.85}\text{Ce}_{0.15}\text{CuO}_4$. As can be seen, the major signature of reconstruction can be described as the band having been “chopped off” above the line A-A (Fig. 3a). Analogous effects can also be found in the energy-momentum intensity distribution for the Eu-LSCO sample [see Fig. 3(b)] thus providing another indication for the FS reconstruction. Besides the discussed signatures of the FS reconstruction, there is also a seeming one-dimensionality in the experimental data. In particular, in Fig. 1 the FS segments parallel to the k_x axis are well pronounced, while their counterparts, which are supposed to be parallel to the k_y axis, are rather diffuse. To check if this might be an evidence for a generic anisotropy in the electronic structure or a mere effect of photoemission matrix elements, we have made similar measurements with the light polarization rotated by 90° . The corresponding FS map and the high symmetry cut $\Gamma_\blacktriangle - \Gamma_0 - \Gamma_\blacktriangledown$ are shown in Figs. 3(c)–(d). As can be seen in Fig. 3c the photoemis-

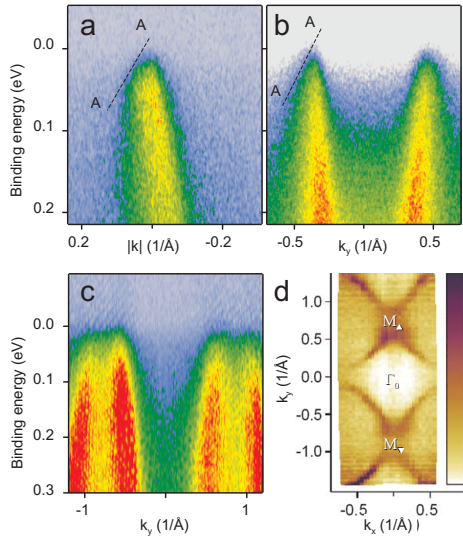


Fig. 3. Effect of the band folding in the spectral function of $\text{Pr}_{1.85}\text{Ce}_{0.15}\text{CuO}_4$ (a) and Eu-LSCO (b). High symmetry cut $\Gamma_{\blacktriangle} - \Gamma_0 - \Gamma_{\blacktriangledown}$ (c) and FS that are supporting a possible FL band crossing along the $\Gamma_{\blacktriangle} - \Gamma_0 - \Gamma_{\blacktriangledown}$ direction. Unlike all the other, the data in panels (c)–(d) were obtained with the inplane component of the light polarization vector parallel to the k_y axis.

sion intensity still remains suppressed in the vicinity of $\Gamma_{\blacktriangle/\blacktriangledown}$ points, which is rather unusual if attributed to unfavorable matrix elements. Moreover, the observed intensity distribution in the $\Gamma_{\blacktriangle} - \Gamma_0 - \Gamma_{\blacktriangledown}$ cut is more consistent with band crossing the FL, rather than with a saddle point expected for stripe-free LSCO system.

One of the first easy-to-grasp consideration of the FS reconstructions due to the spin and charge modulation has been given in Ref. 27, but focusing mainly on the Hall effect the authors restricted the discussion to the formal FS topology. When aiming at comparison to the photoemission experiment such a description needs to be extended, since these are not the bands that are seen directly in the photoemission experiment but the spectral function modified by the photoemission matrix elements $\Delta_{f,i}$. Even when the matrix elements can be neglected in the unreconstructed case, the intensity variations upon the reconstruction are generally tremendous [31]. Typically one notes a significantly lower intensity of the newly sprang-up replicas as compared to the original unreconstructed bands. To understand this important and ubiquitous intensity disparity [30, 31] one may turn to a sudden approximation as the simplest, but still sufficient for this purpose, approach. In this case the intensity of photoelectrons detected at some final state $|f\rangle$ can be written as [32]:

$$J_f(\omega) = f(\omega) \sum_i |\Delta_{f,i}|^2 A_i(\omega) = \sum_i |\Delta_{f,i}|^2 A_i^<(\omega). \quad (1)$$

Here the summation runs over the set of one-electron states $|i\rangle$ forming the basis in which the spectral function $A_i(\omega)$ is given. For our particular purpose, when considering a 2D cuprate, we reduce the complete basis set to states forming the single band crossing the FL, and naturally enumerate

them by the Bloch quasi-momentum $\mathbf{k} = (k_x, k_y)$ limited to the unreconstructed BZ: $k_x \in [-\frac{\pi}{a}; +\frac{\pi}{a}]$, $k_y \in [-\frac{\pi}{b}; +\frac{\pi}{b}]$. Furthermore, we consider the excitations as a well defined quasiparticles and write the Hamiltonian in a diagonal form

$$\hat{H}_0 = \sum_{\mathbf{k} \in \text{BZ}} \varepsilon_{\mathbf{k}} \hat{c}_{\mathbf{k}}^\dagger \hat{c}_{\mathbf{k}}, \quad (2)$$

with $\varepsilon_{\mathbf{k}}$ being the renormalized band dispersion. It is easy to check that the spectral function reduces to a trail of delta functions aligned along the band dispersion [33], and that the matrix element $\Delta_{f,i}$ between the final state $|f\rangle$ characterized by the electron momentum \mathbf{p} and initial state $|i\rangle$ given by the Bloch wave with quasi-momentum \mathbf{k} ensures periodic replication of the photoemission picture determined by $A_{\mathbf{k}}(\omega)$ over different Mahan cones [22] as it can actually be seen in Fig. 1.

As was pointed out in Ref. 27, commensurate stripe order assumed in the model of antiphase stripe domains [26] induces additional potential due to scattering on spin and charge modulations $V = V_s + V_c$ that can be characterised by two most significant matrix elements

$$V_s = \langle \mathbf{k} | \hat{V}_s(\mathbf{r}) | \mathbf{k} \pm \mathbf{Q}_s \rangle, \text{ with } \mathbf{Q}_s = (3\pi/4; \pi), \text{ and} \quad (3)$$

$$V_c = \langle \mathbf{k} | \hat{V}_c(\mathbf{r}) | \mathbf{k} \pm \mathbf{Q}_c \rangle, \text{ with } \mathbf{Q}_c = (\pi/4; 0).$$

The choice of this particular model is motivated by the recent inelastic X-ray and neutron scattering experiments that seem to be in agreement with the theoretically expected vectors of charge modulations, not taking into account a small ($\sim 3\%$) incommensurability [34].

Introducing a quasi-momentum \mathbf{q} limited to the reduced Brillouin zone (RBZ) because of the enlarged unit cell in the real space, and zone number $m = 0, \dots, 7$, which becomes necessary to describe the states of the original band if the RBZ is used, the system Hamiltonian for the modulated case can be written as a matrix with respect to the zone index m :

$$\hat{H} = \sum_{\substack{\mathbf{q} \in \text{RBZ} \\ m,n=0,\dots,7}} (\delta_{m,n} \varepsilon_{\mathbf{q}+\mathbf{g}_m} + V_{m,n}) \hat{c}_{\mathbf{q}+\mathbf{g}_m}^\dagger \hat{c}_{\mathbf{q}+\mathbf{g}_n}, \text{ with}$$

$$V_{m,n}(\mathbf{q}) = \begin{pmatrix} 0 & V_c & 0 & V_c & 0 & V_s & V_s & 0 \\ V_c & 0 & V_c & 0 & 0 & 0 & V_s & V_s \\ 0 & V_c & 0 & V_c & V_s & 0 & 0 & V_s \\ V_c & 0 & V_c & 0 & V_s & V_s & 0 & 0 \\ 0 & 0 & V_s & V_s & 0 & V_c & 0 & V_c \\ V_s & 0 & 0 & V_s & V_c & 0 & V_c & 0 \\ V_s & V_s & 0 & 0 & 0 & V_c & 0 & V_c \\ 0 & V_s & V_s & 0 & V_c & 0 & V_c & 0 \end{pmatrix}, \quad (4)$$

where \mathbf{g}_m is a set of 8 vectors determined by the condition $\mathbf{g}_m = k_m \mathbf{Q}_c + l_m \mathbf{Q}_s \in \text{BZ}$ and $k_m, l_m \in \mathbb{Z}$. Diagonalizing the matrix $H_{m,n}(\mathbf{q}) = \delta_{m,n} \varepsilon_{\mathbf{q}+\mathbf{g}_m} + V_{m,n}$ results in 8 eigenvalues and eigenstates for each particular $\mathbf{q} \in \text{RBZ}$:

$$\hat{H} = \sum_{\substack{\mathbf{q} \in \text{RBZ} \\ i,m,n=0,\dots,7}} D_{m,i}^*(\mathbf{q}) E_i(\mathbf{q}) D_{i,n}(\mathbf{q}) \hat{c}_{\mathbf{q}+\mathbf{g}_m}^\dagger \hat{c}_{\mathbf{q}+\mathbf{g}_n} =$$

$$\sum_{\substack{\mathbf{q} \in \text{RBZ} \\ i=0,\dots,7}} E_i(\mathbf{q}) \hat{a}_{\mathbf{q},i}^\dagger \hat{a}_{\mathbf{q},i}, \text{ where } \hat{a}_{\mathbf{q},i} = \sum_n D_{i,n}(\mathbf{q}) \hat{c}_{\mathbf{q}+\mathbf{g}_n}.$$

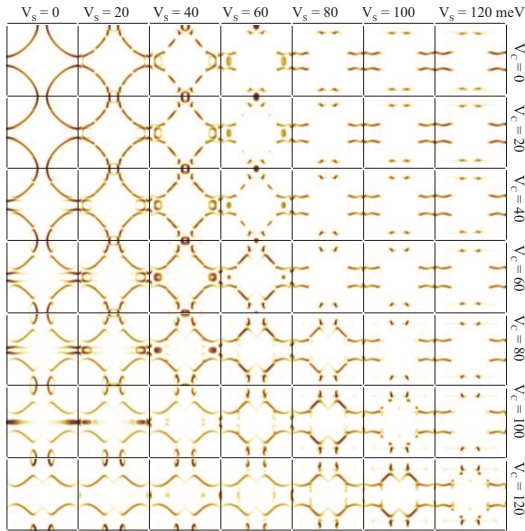


Fig. 4. Calculated FS for various scattering potentials V_c and V_s . Calculated spectral function was smoothed within small energy and momentum windows to simulate experimental resolution.

Now, knowing the eigenstates $\hat{a}_{\mathbf{q},i}^\dagger|0\rangle$ and eigenenergies $E_i(\mathbf{q})$ of the reconstructed system we write the spectral function

$$\begin{aligned}
 A_{\mathbf{k}}^<(\omega) &= \sum_{\substack{\mathbf{q} \in \text{RBZ}, \\ i=0, \dots, 7}} \left| \langle 0 | \hat{c}_{\mathbf{k}} | \mathbf{q}, i \rangle \right|^2 \delta(E_i(\mathbf{q}) - \omega) = \\
 & \sum_{\substack{\mathbf{q} \in \text{RBZ}, \\ i, m=0, \dots, 7}} \left| \langle 0 | \hat{c}_{\mathbf{k}} D_{m,i}^*(\mathbf{q}) \hat{c}_{\mathbf{q}+\mathbf{g}_m}^\dagger | 0 \rangle \right|^2 \delta(E_i(\mathbf{q}) - \omega) = \\
 & \sum_{\substack{\mathbf{q} \in \text{RBZ}, \\ i, m=0, \dots, 7}} \left| D_{m,i}^*(\mathbf{k} - \mathbf{g}_m) \right|^2 \delta(E_i(\mathbf{k} - \mathbf{g}_m) - \omega).
 \end{aligned} \quad (6)$$

From the last formula it can be easily seen that for the case of infinitesimally small potential $V_{n,m}(\mathbf{q})$ the reconstructed band structure must consist of 8 “replicas” obtained from the original structure shifted by vectors \mathbf{g}_m with the distribution of the spectral weight determined by the components of eigenvectors $D_{m,i}(\mathbf{k} - \mathbf{g}_m)$, which results in an infinitesimally small intensity of all the replicas that do not overlap with the original structure. In case of scattering potential values comparable to the band width of the original structure the general property of weak replica intensities remains valid, though the simple “rule of shifts” breaks down and the evaluation of the spectral function must be done numerically.

To check whether the experimental FS can be reproduced within the discussed model, we have calculated the spectral weight distributions for different spin and charge scattering potentials. For the unreconstructed band dispersion $\varepsilon_{\mathbf{k}} = \varepsilon_0 - 2t(\cos k_x + \cos k_y) - 4t' \cos k_x \cos k_y - 2t'' \cos 2k_x \cos 2k_y$ we used experimental data published for pure LSCO system [28], interpolating between doping levels $x = 0.07$ and 0.15 and adjusting the chemical potential

to obtain precise doping level of $x = 0.125$, which results in the following parameters: $\varepsilon_0 = 0.175$, $t = 0.25$, $t' = -0.04$, and $t'' = 0.02$ eV. The obtained distributions are shown in Fig. 4. Before comparing the calculated FS to the experimental one we have to mention that in the model we have preserved the anisotropy of the stripe scattering potential, while in the experimental data one is likely to observe coexistence of stripes running along the x and y direction. Thus when searching for the optimal values of $V_{s,c}$ we should not sift out the calculated spectra just because of their one-dimensionality. From the Fig. 4 it is obvious that there is no problem for the model to reproduce the seeming octagonal structure of the experimental FS, though the values of spin scattering exceeding 80 meV are surely too large. Further restriction on the values of $V_{s,c}$ can be drawn comparing distances between the most intense part in the intensity distributions. Our subjective judgement for the nearest fit to the experimental data would be the case of $V_s \approx 60 \pm 20$ and $V_c \approx 100 \pm 20$ meV.

When further comparing the model to the the experimental data the issue of the stripe scattering potential periodicity has to be mentioned. This seems to be especially important for the problem of a pseudogap that has been observed in a similar type of stripe compound [21]. Strictly speaking both charge and spin order are not commensurate to the lattice and have finite correlation lengths [34], which certainly must affect the finer details in the electronic structure. It has been known for decades from studies of quasicrystals and quasi-periodic alloys that incommensurate potentials generally lead to suppression of the spectral weight at the FL, which in that field of research has also been termed as “pseudogap” [35, 36, 37]. Moreover there are known successful attempts to transfer the ideas developed for the quasicrystals onto the problem of mysterious pseudogap in cuprates [38]. Recently a pseudogap effect, similar to the one discussed in high- T_c cuprate, has been detected in the incommensurate phase of CDW bearing compound [31] TaSe₂ once again suggesting that the incommensurate order might be a long sought common origin of the pseudogaps. Unfortunately a precise calculation of rational approximates to the incommensurate structure is encumbered with drastically increased numeric complexity, although it is obvious that such a calculation would significantly help to understand the pseudogap formation mechanism in high-temperature superconducting cuprates.

This project is part of the Forschergruppe FOR538 and is supported by the DFG under Grants No. KN393/4 and BO1912/2-1. We thank R. Hübel for technical support.

-
- [1] S. A. Kivelson *et al.*, Rev. Mod. Phys. **75**, 1201 (2003).
 - [2] A. H. Castro Neto and C. Morias Smith, arXiv:cond-mat/0304094; *Strong Interactions in Low Dimensions*, D. Baeriswyl and L. Degiorgi, eds. (Kluwer, 2004), p. 277.
 - [3] M. Vojta, Phys. Rev. B **66**, 104505 (2002).

- [4] I. Martin *et al.*, Europhys. Lett., **56**, 849 (2001).
- [5] K.M. Kojima *et al.*, Physica B **289**, 343 (2000).
- [6] H.-H. Klauss *et al.*, Phys. Rev. Lett. **85**, 4590 (2000).
- [7] A. W. Huntet *et al.*, Phys. Rev. Lett. **82**, 4300 (1999).
- [8] G. B. Teitelbaum, B. Büchner, and H. de Gronckel, Phys. Rev. Lett. **84**, 2949 (2000).
- [9] V. Kataev *et al.*, Phys. Rev. B **58**, R11876 (1998).
- [10] B. J. Suh *et al.*, Phys. Rev. B **61**, R9265 (2000).
- [11] B. Simovič *et al.*, Phys. Rev. B **68**, 012415 (2003).
- [12] J. M. Tranquada *et al.*, Nature **375**, 561 (1995).
- [13] J. M. Tranquada *et al.*, Phys. Rev. Lett. **78**, 338 (1997).
- [14] J. E. Hoffman *et al.*, Science **295**, 466 (2002).
- [15] M. Vershinin *et al.*, Science **303**, 1995 (2004).
- [16] D. LeBoeuf *et al.*, Nature **450**, 533 (2007).
- [17] T. Adachi *et al.*, Phys. Rev. B **64**, 144524 (2001).
- [18] Y. Nakamura and S. Uchida Phys. Rev. B **46**, 5841 (1992).
- [19] S. E. Sebastian *et al.*, Nature **454**, 200 (2008).
- [20] X. J. Zhou, *et al.*, Science **286**, 268 (1999).
- [21] T. Valla, *et al.*, Science **314**, 1914 (2006).
- [22] G. D. Mahan, Phys. Rev. B **2**, 4334 (1970).
- [23] V. B. Zabolotny *et al.*, Phys. Rev. B **76**, 024502 (2007).
- [24] D. S. Inosov *et al.*, Phys. Rev. B **77**, 212504 (2008).
- [25] S. V. Borisenko *et al.*, Phys. Rev. B **64**, 094513 (2001).
- [26] J. Zaanen and O. Gunnarsson, Phys. Rev. B **40**, 7391 (1989).
- [27] A. J. Millis, M. R. Norman, Phys. Rev. B **76**, 220503(R) (2007).
- [28] T. Yoshida *et al.* Phys. Rev. B **74**, 224510 (2006).
- [29] S. R. Park *et al.*, Phys. Rev. B **75** 060501(R) (2007).
- [30] V. Brouet *et al.*, Phys. Rev. Lett. **93** 126405 (2004).
- [31] S. V. Borisenko *et al.* Phys. Rev. Lett. **100**, 196402 (2008).
- [32] L. Hedin, J. D. Lee, J. El. Spectroscopy and Rel. Phenomena, **123**, 289 (2002).
- [33] G. D. Mahan, Many particle physics., Plenum Press, 1981.
- [34] Y.-J. Kim, G. D. Gu, T. Gog, and D. Casa Phys. Rev. B **77**, 064520 (2008).
- [35] X. Wu *et al.* Phys. Rev. Lett. **75**, 4540 (1995).
- [36] J. Hafner and M. Krajčí Phys. Rev. Lett. **68**, 2321 (1992).
- [37] K. Ueda and H. Tsunetsugu, Phys. Rev. Lett. **58**, 1272 (1987).
- [38] G. Seibold *et al.*, Eur. Phys. J. B **13**, 87 (2000); arXiv:cond-mat/9906108.